

The dominant terms in the differential and total cross sections for the considered processes coincide with the corresponding formulas obtained by Gorshkov, Mikhailov, and Sherman<sup>[8]</sup> for the photon-energy region  $\eta \ll \omega \ll m$ .

The above-given formulas allow us to calculate the cross sections for the indicated scattering processes in the region of energies  $\omega \gg \eta$  for small and medium  $Z$  (up to  $Z \sim 50$ ); for large  $Z$  the higher-order terms discarded in the cross sections should be taken into account.

The authors thank V. G. Gorshkov for useful discussions.

<sup>1</sup>M. Gavril, Phys. Rev. **163**, 147 (1967).

<sup>2</sup>B. A. Zon, N. L. Manakov, and L. P. Rapoport, Zh. Eksp. Teor. Fiz. **55**, 924 (1968) [Sov. Phys. JETP **28**, 480 (1969)].

<sup>3</sup>S. I. Vetchinkin and S. V. Khristenko, Opt. Spektrosk. **25**, 650 (1968) [Opt. Spectrosc. **25**, 365 (1968)].

<sup>4</sup>Ya. I. Granovskii, Zh. Eksp. Teor. Fiz. **56**, 605 (1969)

[Sov. Phys. JETP **29**, 333 (1969)].

<sup>5</sup>V. S. Polikanov, Preprint FTI-320, Leningrad, 1970.

<sup>6</sup>A. I. Ignat'ev, Preprint LIYaF-102, Leningrad, 1974.

<sup>7</sup>V. G. Gorshkov and V. S. Polikanov, Pis'ma Zh. Eksp. Teor. Fiz. **9**, 464 (1969) [JETP Lett. **9**, 279 (1969)].

<sup>8</sup>V. G. Gorshkov, A. I. Mikhailov, and S. G. Sherman, Zh. Eksp. Teor. Fiz. **66**, 2020 (1974) [Sov. Phys. JETP **39**, 995 (1974)].

<sup>9</sup>G. E. Brown, R. E. Peierls, and J. B. Woodward, Proc. Roy. Soc. **A227**, 51 (1955); S. Brenner, G. E. Brown, and J. B. Woodward, Proc. Roy. Soc. **A227**, 59 (1955); G. E. Brown and D. E. Mayers, Proc. Roy. Soc. **A242**, 89 (1957).

<sup>10</sup>I. B. Whittingham, J. Phys. **A4**, 21 (1971).

<sup>11</sup>V. G. Gorshkov, A. I. Mikhailov, V. S. Polikanov, and S. G. Sherman, Phys. Lett. **30A**, 455 (1969).

<sup>12</sup>V. G. Gorshkov, A. I. Mikhailov, and S. G. Sherman, Zh. Eksp. Teor. Fiz. **64**, 1128 (1973) [Sov. Phys. JETP **37**, 572 (1973)].

<sup>13</sup>V. G. Gorshkov, A. I. Mikhailov, and V. S. Polikanov, Nucl. Phys. **55**, 273 (1964).

<sup>14</sup>A. I. Mikhailov and S. G. Sherman, Zh. Eksp. Teor. Fiz. **69**, 1888 (1975) [Sov. Phys. JETP **42**, 958 (1976)].

Translated by A. K. Ageyi.

## Excitation of large-amplitude solitary waves in a plasma

V. D. Fedorchenko, Yu. P. Mazalov, A. S. Bakaĭ, A. V. Pashchenko, and B. N. Rutkevich

*Physico-technical Institute, Ukrainian Academy of Sciences*

(Submitted October 26, 1975)

Zh. Eksp. Teor. Fiz. **70**, 1768-1778 (May 1976)

A method is developed for generating solitary space charge waves in a plasma by employing an electron beam that is strongly modulated in velocity. At a current of 7 mA, mean beam energy 200 eV, and modulation depth  $\sim 0.5$ , solitons with a mean velocity of  $3.3 \cdot 10^9$  cm/sec and amplitude up to 2 kV can be generated by the method. The amplitude attained is about 0.65 of the amplitude limit at which the plasma electrons are trapped. The details of the soliton generation process are elucidated. It is shown, in particular, that the fast beam electrons whose energy exceeds the mean value transfer to the solitons an energy proportional to the modulation depth. The effect of varying the beam and plasma parameters as well as the geometrical dimensions of the plasma on soliton formation is investigated.

PACS numbers: 52.40.Mj

### INTRODUCTION

Excitation of large-amplitude space-charge waves is of great interest for applications such as particle acceleration, plasma heating, and others. At a given propagation velocity  $w$  it is possible to excite in the plasma a wave with amplitude  $\varphi_m$  not exceeding a value

$$\varphi_m = mw^2/2e \quad (1)$$

( $e$  and  $m$  are the charge and mass of the electron), such that the wave begins to capture the plasma electrons. (We neglect here the thermal velocity of the electrons, which we assume to be small in comparison with  $w$ .) However, the wave can become essentially nonlinear at amplitudes much lower than  $\varphi_m$ . As follows from the theory of stationary waves in a plasma layer or cylinder,<sup>[1]</sup> the space-charge waveform is sinusoidal only at low amplitudes, and in the limit of

large amplitudes the wave goes over into solitary waves (solitons), the amplitudes of which can reach values  $\varphi_m$ .

Excitation of solitons in a bounded plasma was investigated experimentally in<sup>[2-5]</sup>. In<sup>[2-4]</sup> the excitation was produced by applying voltage pulses to an electrode immersed in the plasma. Another method of soliton excitation is described in<sup>[5]</sup>, where the effect was obtained in a beam-plasma system by modulating the initial beam velocity.

The present paper is devoted to a further investigation of the formation and propagation of solitons in a beam-plasma system. With rather modest means (initial beam energy 200 eV, current 7 mA), the soliton amplitude, as shown by measurements, reaches 2 kV at a propagation velocity  $3.3 \times 10^9$  cm/sec. This gives grounds for hoping that for moderate beam parameters it is possible to excite in this manner solitons that are of practical interest.

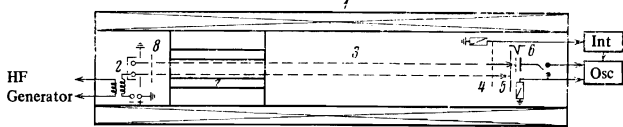


FIG. 1. Diagram of installation: 1) Solenoid, 2) electron gun, 3) electron beam, 4) movable probe, 5) collector, 6) electrostatic analyzer, 7) channel in which the pressure drop is produced, 8) control grid, Int—integrator, Osc—oscilloscope.

## GENERATION AND INVESTIGATION OF SOLITONS

The experimental investigations of the interaction of modulated electron beams in a plasma were carried out with the installation illustrated in Fig. 1.

A hollow electron beam of 0.5 cm diameter passes through a metallic tube of 9 cm diameter placed in a homogeneous magnetic field  $H=400$  Oe. The electrons are injected by gun 2. The electron emitter is a tungsten filament 0.05 cm thick. The average beam energy is 200–300 eV and the current is 7 mA. The pressure is  $2 \times 10^{-4}$  Torr in the working region and lower by one order of magnitude in the cathode region. The pressure drop is ensured by channel 7 and by air admitted in the working part of the chamber. The plasma is produced by ionization of the gas with an electron beam. The accelerating voltage is modulated by oscillations from a generator of frequency  $f$  in the range 5–15 MHz applied through a transformer connected to the cathode of the gun 2. The modulation amplitude could reach 100 V. At all modulation amplitudes, the gun operated in the saturation regime so that the beam was only velocity modulated. The electrons are bunched in channel 7 (50 cm long).

The interaction of the bunched beam with the plasma was investigated with a moving probe 4 in the form of a tungsten grid with transparency 95% and diameter 2 cm. The signal from the probe was fed through a broadband amplifier, integrated, and applied to an oscilloscope.

An electrostatic analyzer 6 was used to plot the en-

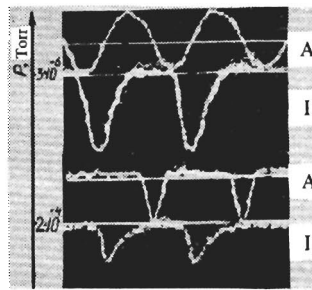


FIG. 3. Oscillations in the circuit of the moving probe (A) and of the collector (I) at pressures  $3 \times 10^{-6}$  Torr (upper pair of oscillograms and  $2 \times 10^{-4}$  Torr (lower pair). Oscillograms A and I characterize the variation of the electric field in the plasma and of the current in the electron beam, respectively.  $U_0=200$  V,  $\bar{U}=70$  V,  $f=10$  MHz,  $L=60$  cm.

ergy distribution of the beam electrons. To this end, a sawtooth retarding voltage of 500 V amplitude was applied to the analyzer grid. The signal from the analyzer collector was differentiated and was applied to the oscilloscope.

The waveform of the registered oscillations depends essentially on the gas pressure in the system, i.e., on the density of the plasma produced by the beam (Fig. 2). At low pressures ( $p=3 \times 10^{-6}$  Torr) the oscillations are close to sawtooth in shape. With increasing pressure, the waveform becomes distorted and at  $p=2 \times 10^{-4}$  Torr the wave turns into a sequence of negative pulses. The distance between the pulses greatly exceeds their width, so that they actually constitute a train of solitons. One soliton is produced in each period of modulation.

At  $p=2 \times 10^{-4}$  Torr in the system beam-plasma instability has its maximum growth rate in the absence of modulation at the frequency 125 MHz. At a beam velocity  $v=8.5 \times 10^8$  cm/sec, the phase velocity of the plasma oscillations is  $7 \times 10^8$  cm/sec. These data enable us to estimate the plasma density at  $n_0=2.9 \times 10^9$  cm $^{-3}$ .

With increasing beam energy, the frequency of the excited oscillations is decreased, while the velocity increases. At high energies, the system becomes stable. The largest beam energy at which the beam-plasma instability still takes place is 800 V, corresponding to a velocity  $1.7 \times 10^9$  cm/sec. It should be close to the maximal velocity of the plasma oscillations, equal to  $\omega_p/k_r$ , where  $k_r$  is the radial component of the wave vector. Knowing  $\omega_p^2=4\pi e^2 n_0/m$ , we obtain  $k_r=0.56$ .

The source of the soliton energy is, naturally, the electron beam. Its energy make up at the exit from the system is strongly altered by the transition to the soliton-generation regime. Figure 3 shows the readings of probe 4 (Fig. 1), as well as oscillograms of the ac component of the current in the electron beam striking the collector 6 (Fig. 1). The oscillograms were taken at pressures  $3 \times 10^{-6}$  and  $2 \times 10^{-4}$  Torr. In the former case no solitons are produced and the probe registers bipolar oscillations. The current is well bunched

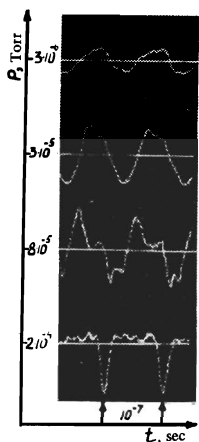


FIG. 2. Waveform of the oscillations in the circuit of the moving probe as a function of the pressure in the chamber. The average electron energy is  $U_0=200$  V, the modulation amplitude is  $U=100$  V, and the modulation frequency is  $f=10$  MHz. The distance from the probe to the end of the transition channel is  $L=60$  cm.

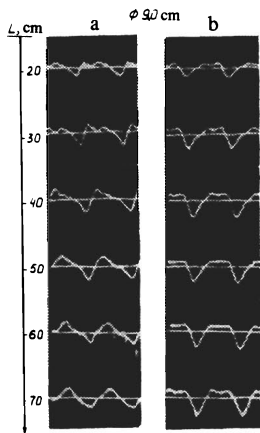


FIG. 4. Oscillations produced in the plasma by a beam of decelerated (a) and accelerated (b) particles.  $U_0 = 300$  V,  $\tilde{U} = 70$  V,  $f = 10$  MHz.

in this case. In the second case, when the probe registers solitary waves, the amplitude of the current modulation in the beam is noticeably decreased.

Further investigations with the aid of an electrostatic analyzer have shown that the residual bunching is due to electrons that are slowed down in the course of the beam modulation. The accelerated part undergoes debunching, probably as a result of the change of the energy spectrum of this part of the beam. The change of the spectrum is a consequence of the interaction of the electrons with the solitary waves. This conclusion allows us to assume that only accelerated electrons take part in the soliton formation.

A direct verification of this assumption is possible if beams consist either of only accelerated or of only slowed-down particles. A beam of accelerated electrons is obtained by applying to the special control grid 8 (Fig. 1) a potential corresponding to the average beam energy. All the slowed-down electrons were reflected by this potential. To remove the accelerated particles, a more complicated method was used, wherein an alternating potential, which retarded the electrons only in the accelerating phase of the modulating signal, was applied to the control grid. As seen from the oscillograms of Fig. 4, solitons are formed only in the beam of accelerated electrons.

Figure 5 shows the results of an analysis of the energy composition of the beam as it emerges from the

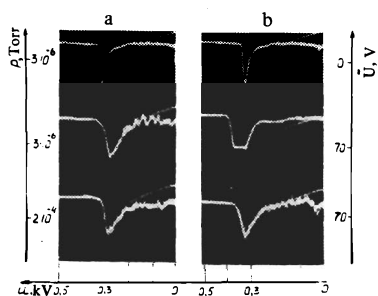


FIG. 5. Energy distribution of the electrons in beams of decelerated (a) and accelerated (b) electrons.  $U_0 = 300$  V,  $\tilde{U} = 70$  V,  $f = 10$  MHz,  $L = 60$  cm, dia. 9 cm.

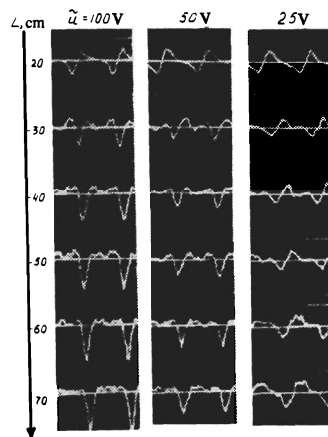


FIG. 6. Evolution of the wave profile at different amplitudes of the modulating voltage.  $U_0 = 200$  V,  $f = 10$  MHz, diameter 9 cm.

system. The upper oscillograms constitute the distribution of the electron energies in the unmodulated beam. The middle oscillograms show the distribution in the beams of the decelerated and accelerated electrons at a pressure  $3 \times 10^{-6}$  Torr, when no solitons are produced. The lowest traces show the distribution in the same beams at a pressure  $2 \times 10^{-4}$  Torr, at which solitons are generated. It is seen that the spectrum of the decelerated particles undergoes only the spreading, characteristic of two-stream instability, towards the lower energies. The change of the spectrum of the accelerated particles is of different character. In the soliton-generation regime, the energy of the accelerated particles decreases and approaches the average energy  $U_0$ . Thus, the experimental data demonstrate that the process of formation of solitary waves is strongly influenced only by the accelerated part of the beam, which transfers to the wave the energy acquired by it to the modulation during the accelerating part of the period. It follows therefore that deep modulation of the beam is necessary in order for solitary waves of appreciable amplitude to be generated. Besides the energy, the modulation depth determines also the length over which the bunching takes place. The role of the depth of modulation is demonstrated by the oscillograms of the signals from the moving probe (Fig. 1) obtained at different distances  $L$  from the end of the transition channel at modulating-voltage amplitudes  $U$  equal to 100, 50, and 25 V (Fig. 6).

At an amplitude 100 V, fully shaped solitons are produced at distances  $L = 30-40$  cm. This distance increases at  $\tilde{U} = 50$  V, and the amplitude of the solitons turns out to be much lower. At  $\tilde{U} = 25$  V, no solitons are produced in the system.

Reduction of the probe-signal oscillograms makes it possible to plot the amplitude and the velocity of the solitary waves against the distance  $L$  (Fig. 7). Both quantities increase rapidly to certain values that subsequently level off. The soliton velocity, which is initially close to the average beam velocity, then increases by almost three times (at  $\tilde{U} = 100$  V) and greatly exceeds

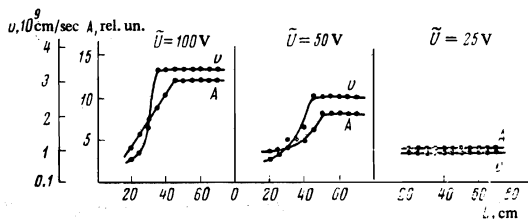


FIG. 7. Dependence of the amplitude  $A$  and of the velocity  $v$  of the solitary wave on the distance  $L$  at different amplitudes of the modulating voltage.  $U_0 = 200$  V,  $f = 10$  MHz, dia. 9 cm.

the velocity of the fastest electrons of the modulated beam. Thus, even in the early stage of the evolution, the solitons move more rapidly than the beam electrons, and they arrive at the end point of the system, as can be judged from Fig. 3, some 50 nsec earlier than the electron bunches. Under certain conditions, the soliton overtakes the electron bunch of the preceding period. This leads to destruction of the soliton.

The amplitude and velocity of the solitary wave, just as the character of their evolution, depend on the diameter of the metallic jacket that surrounds the plasma column. All the experiments mentioned above were performed at a jacket diameter 9 cm. Figure 8 shows results of experiments with tubes of smaller diameters. At 4.5 cm diameter, the amplitude and velocity of the soliton initially increase, but even at  $L = 50-60$  cm the characteristic contour of the soliton is deformed and assumes the sawtooth shape usually observed at low pressure. At 3.0 cm diameter, the soliton decay process occurs earlier, at  $L = 30-40$  cm.

With decreasing jacket diameter, the propagation velocity of the solitons excited by the modulated beam decreases. The same is observed with decreasing pressure in the chamber.

The next experiment was aimed at an absolute measurement of the soliton amplitude. To this end, a probing beam method was used, based on the fact that the character of the interaction of the beam of velocity  $v$  with a soliton having an amplitude  $\phi_m$  and a velocity  $w$  is rapidly changed when  $(w-v)^2 - 2e\phi_m/m = 0$ . Thus  $(w-v)^2 > 2e\phi_m/m$  the electrons of the probing beam pass through the soliton without changing their direction of motion, whereas if the inequality is reversed they are reflected by the soliton field. In other words, electrons with velocities in the interval  $[v_1, v_2]$ , where  $v_{1,2} = w \pm (2e\phi_m/m)^{1/2}$ , are captured by the wave. The capture of the electrons of the probing beam by a sequence

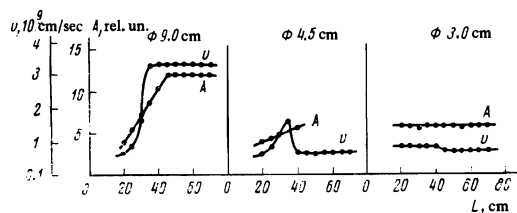


FIG. 8. Dependence of the amplitude and velocity of a solitary wave on the distance  $L$  at different diameters of the metallic jacket.  $U_0 = 200$  V,  $\tilde{U} = 100$  V,  $f = 10$  MHz.

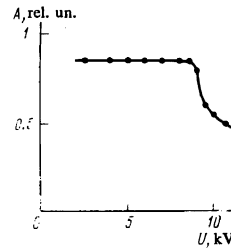


FIG. 9. Dependence of the amplitude of the probing-beam modulation on the beam energy.

of solitons leads to deep modulation of the beam current measured at the exit from the system. Indeed, as shown by experiment, modulation is always present, but is much deeper in the capture regime.

The measurements were performed under the following conditions: the energy of main beam  $U_0 = 200$  V, current 7 mA, and modulation amplitude  $\tilde{U} = 100$  V. The probing beam was directed along the system axis in the direction of the main beam. Its diameter was 0.2 cm, its current 100  $\mu$ A, and the energy could be increased to 11 kV.

The measurements have shown that at the end point of the system, in the soliton generation regime, the probing-beam current is modulated at the modulation frequency of the main beam. With increasing probing-beam energy, the amplitude of the current modulation near 10 kV decreases abruptly (Fig. 9). Identifying this energy with the quantity  $mv_0^2/2$ , it is easy to obtain an estimate of the maximum potential. It is close to 2 kV.

## SOME THEORETICAL RESULTS

The possible existence of solitary space-charge waves was theoretically demonstrated in [1,2]. Solitons were analyzed in [2,6] for the case of cylindrical plasma at an arbitrary intensity of the external longitudinal magnetic field. The case of a plasma filament of small diameter,  $a \ll b \ll L_0$  ( $a$ —filament radius,  $b$ —metallic jacket radius,  $L_0$  wavelength of space charge) was considered in [1] under the assumptions that the magnetic field is strong,  $\omega_p \ll \omega_H$  ( $\omega_H$  is the electron-cyclotron frequency). In this case the equations of motion and the Poisson equations take the form

$$\frac{\partial v}{\partial t} + v \frac{\partial v}{\partial z} = -\frac{e}{m} \frac{\partial \phi}{\partial z}, \quad (2)$$

$$\frac{\partial n}{\partial t} + \frac{\partial}{\partial z} (nv) = 0, \quad (3)$$

$$\frac{d^2 \phi}{dz^2} = 4\pi e (n_0 - n) + \kappa \phi, \quad (4)$$

where  $v$  and  $n$  are the velocity and density of the plasma electrons,  $\kappa$  is the transverse component of the wave vector:  $\kappa^2 \approx 2[a^2 \ln(b/a)]^{-1}$ .

The foregoing equations have a solution in the form of solitary waves propagating with constant velocity  $w$ . The electric potential  $\phi$  satisfies in this case the equation

$$\left( \frac{d\phi}{d\xi} \right)^2 = \Phi^2 + \frac{4\Phi}{\sigma^2} - \frac{9}{\sigma^2} (1 - \sqrt{1 - \Phi}), \quad (5)$$

where

$$\Phi = 2 \frac{e}{m} \frac{\Phi}{\omega^2}, \quad \xi = \kappa(z - \omega t), \quad \sigma = \kappa \omega / \omega_p, \\ \omega_p^2 = 4\pi e^2 n / m.$$

The distribution of the potential in the wave takes the form of a solitary pulse, the amplitude of which is connected with the parameter  $\sigma$  by the relation

$$\Phi_m = 4(\sigma - 1) / \sigma^2. \quad (6)$$

The amplitude  $\Phi_m$  can take on arbitrary values in the interval (0, 1), which corresponds to an interval of  $\sigma$  from 1 to 2. It follows from (6) that the soliton velocity increases with increasing amplitude. The velocity of a soliton of vanishingly small amplitude is equal to the largest possible propagation velocity of the small oscillations of the space-charge waves in the plasma column, and is equal to  $\omega_p / \kappa$ . The maximum possible velocity corresponding to the limiting amplitude  $\varphi_m$  (1) is twice as large:  $w_m = 2\omega_p / \kappa$ .

The shape of the soliton is determined by the formula

$$\varphi = \varphi_m / \text{ch}^2 [k(z - \omega t)], \quad (7)$$

where  $k = (1/2)\sqrt{1 - \sigma^2}$ . The width of the soliton (at a height equal to half its amplitude) is represented by the expression

$$\Delta = 3.5 / \kappa \sqrt{1 - \sigma^2}. \quad (8)$$

The soliton has a characteristic peaked shape. The point with the maximum field intensity lies quite close to the vertex. The potential at this point is determined by the equation

$$\Phi(E_{\text{max}}) = 1/2 - 2\sigma^2 + \sqrt{1/4 + 2\sigma^2}.$$

As  $\sigma \rightarrow 1$  its value is  $2\Phi_m/3$ , and as  $\sigma \rightarrow 2$  we have  $\Phi(E_{\text{max}}) = 0.87$ . In the latter case ( $\sigma = 2$ ) the maximum electric field intensity is  $0.59 \kappa \varphi_m$ .

A remarkable property of certain nonlinear equations, and in particular of the Korteweg-de Vries equation, to which the system (2)–(4) can be approximately reduced (see [2]), is that the solitons are for these equations stable solutions into which initial perturbations of rather general type decay asymptotically. This means that if the initial perturbation resembles the soliton (7) even remotely, then in the course of time there will be separated from it a soliton and a certain residue, which is customarily called the "oscillatory tail." Consequently, excitation of solitons in systems whose motion satisfies the Korteweg-de Vries equation can be effected relatively simply.

## DISCUSSION OF EXPERIMENTAL RESULTS

The dynamics of excitations of solitons that are velocity modulated by a beam in a plasma goes through several stages. First, the modulated-beam particles, moving in the vacuum channel 7 (Fig. 1), become

bunched. Entering the plasma, the bunched beam excites a periodic potential wave with which it interacts. As a result of this interaction, the fast part of the beam particles transfers an appreciable fraction of the energy of the wave within a short time and is slowed down. The slow electrons do not interact effectively with the wave for a relatively long time, long enough for the soliton to be formed. The interaction of the soliton with the decelerated particles is accompanied by transfer of energy to the latter and it leads to breakup of the soliton. If the characteristic time  $\tau_*$  of the interaction of the soliton with the slow particles is longer than the time of flight  $\tau_0$ , of the solitons through the plasma column and the time of formation of the soliton is shorter than  $\tau_0$ , then almost stationary solitons can be observed at the end of the plasma column.

Let us discuss each of the soliton-excitation stages in greater detail.

The degree of bunching of the electrons entering the plasma at the end point of the vacuum channel can be conveniently estimated with the aid of the coefficient  $\eta$ , which is the ratio of the wavelength  $L_0 = 2\pi \bar{v}_b / \omega_0$  ( $\bar{v}_b$  is the average beam velocity,  $\omega_0$  is the modulation frequency) to the average length of the electron bunch. The bunching coefficient  $\eta$  reaches a maximum at the point where the electron trajectories begin to intersect. The distribution of the beam charge can be approximated by a piecewise-constant function:

$$n_0(\xi) = \begin{cases} 0, & 0 < \xi < L_0(1 - \eta^{-1}), \\ \eta n_{0b}, & L_0(1 - \eta^{-1}) < \xi < L_0, \end{cases} \quad (9)$$

where  $n_{0b}$  is the average beam density and  $\xi = x - \bar{v}_b t$ . The electric field excited by the inhomogeneous beam (9) with compensated charge can be easily obtained from the Poisson equation

$$E(\xi) = \begin{cases} 4\pi n_{0b} \xi, & 0 < \xi < L_0(1 - \eta^{-1}), \\ 4\pi n_{0b} [(\eta - 1)(L_0 - \xi)], & L_0(1 - \eta^{-1}) < \xi < L_0. \end{cases} \quad (10)$$

It has a sawtooth shape with a steep leading front (its width is equal to  $L_0 \eta^{-1}$ ) and a gently sloping trailing edge, (of width  $L_0(1 - \eta^{-1})$ ). Sawtooth waves are observed at the beginning of the system, as seen from Fig. 6. The amplitude of the plasma wave excited by a beam having a density distribution (9) at the beginning of the plasma column is smaller by an approximate factor  $\sqrt{2}$  than the amplitude of the wave in the absence of the plasma (10), inasmuch as half the energy of the plasma wave is contained in the plasma-electron oscillations.

Essential characteristics of the initial perturbation are the ratio  $\omega_p / \omega_0$ , of the plasma frequency to the modulation frequency, and the number of harmonics with comparable amplitudes. It is known that the waves with frequencies lower than  $\omega_p$  are amplified in bounded beam-plasma systems. Since the solitons are formed as a result of the interactions of harmonics with one another, it is clear that this process is faster the closer the number  $N_0$  of harmonics of the initial perturbation to the number  $N_s$  of harmonics of the formed soliton and the larger their amplitudes. At  $N_0 \approx N_s$  and  $N_0 \omega_0$

$< \omega_p$ , all the harmonics of the initial perturbations are amplified in the beam-plasma interaction process, and this leads to a rapid formation of the solitons. At  $\omega_0 \sim \omega_p$ , only the first harmonics are amplified in the plasma, and the formation of the soliton becomes difficult. The experimental results confirming this conclusion are shown in Fig. 3, from which it is seen that at low pressures  $p = 3 \times 10^{-6}$  Torr, when  $\omega_0 \sim \omega_p$ , in spite of the fact that the beam particles are well bunched, the wave has an almost sinusoidal shape. At higher pressure  $p = 2 \times 10^{-4}$  Torr, when  $\omega_p \gg \omega_0$ , a train of solitons with a large number of multiple harmonics is produced in the system. It is seen from (9) and (10) that  $N_0 \sim \eta$  and consequently the better the beam is bunched on entering the plasma, the larger is the number of harmonics contained in the initial perturbation and the faster is the soliton formation. This is confirmed by experimental results shown in Fig. 6, where it is seen that it is impossible to observe soliton formation in the system at a low modulation depth ( $\bar{U} = 25$  V), when no electron trajectory intersections occur over the length of the vacuum channel ( $\sim 50$  cm) (the intersection takes place at  $\bar{U} \sim 100$  V) and the bunching coefficient  $\eta$  and hence the number of harmonics  $N_0$  are small.

In the next stage of soliton excitation the beam particles, interacting with the wave excited by them, transfer energy to the wave. Let us examine this process in greater detail and estimate the energy transferred by the beam particles to the wave. Let  $\omega_p \gg \omega_0$  and  $\eta \gg 1$ , so that the beam is well bunched as it enters the plasma and the waveform is approximated by expression (10). It is seen from (9) and (10) that in this case the group of electrons is located behind the minimum of the potential, at an average distance  $L\eta^{-1}/2$  from the steep leading front of the wave. Consequently, the fast electrons, moving with velocities  $v > v_{ph}$  larger than the phase velocity of the wave, are reflected within a time  $\tau_* = (1/2)L_0\eta^{-1}(2e\bar{U}/m)^{-1/2}$  from the steep front, transferring at the same time to the wave an energy

$$\mathcal{E}_* \approx \frac{1}{2} n_{0e} e \bar{U}. \quad (11)$$

We assume here that the number of fast electrons is equal to the total number of the beam electrons. The slow electrons with velocities lower than the phase velocity of the wave are accelerated by the waves on reflection from the gently sloping trailing edge of the wave, but the average time in which this takes place is obviously equal to

$$\tau_- = L_0(1-\eta^{-1})(2e\bar{U}/m)^{-1/2},$$

i.e., it is  $\eta - 1$  times longer than the time  $\tau_*$  during which the fast particles are reflected. Consequently, in the time interval  $\tau_* < t < \tau_-$  the wave has a maximum

energy approximately equal to  $\mathcal{E}_*$ , which is proportional, as seen from (11), to the density and depth of modulation of the beam. The length  $l$  of the plasma column is in our system 70 cm,  $L_0 \approx 2 \times 10^2$  cm,  $\bar{U} \approx 100$  V,  $N_0 \approx \eta \approx 12$ ,<sup>[5]</sup> the soliton velocity is  $w \approx 10^9$ , and consequently the time of flight of the soliton through the system is  $\tau_0 \approx 7 \times 10^{-8}$  sec,  $\tau_* \approx 2.5 \times 10^{-8}$  sec, and  $\tau_- \approx 3 \times 10^{-7}$  sec. We see that  $\tau_* < \tau_0 < \tau_-$ , and consequently the fast particles transfer within a short time to the wave an energy  $\mathcal{E}_*$ , whereas the slow particles do not have time to alter noticeably the wave energy over the length of the system. Since the average particle velocity relative to the wave is  $8 \times 10^8$  cm/sec at  $\bar{U} \approx 100$  V, the fast particles transfer energy to the wave over a distance 20 cm from the start of the plasma column.

In the next stage, when the interaction of the wave with the particles is negligible, the evolution of the wave is governed by the nonlinear interaction between the harmonics and leads to formation of a soliton if the formation time is shorter than  $\tau_0$ . Since the rate of this process, as seen from the equations of motion (2)–(5), is proportional to the energy of the wave, the formation of the soliton should take place at  $t > \tau_*$  over distances  $L > 20$  cm, and should be faster the larger  $\mathcal{E}_*$ . This is precisely what we have observed in experiment. It is seen from Fig. 7 that at  $\bar{U} = 100$  V the formation of the soliton takes place over a distance approximately half as large as at  $\bar{U} = 50$  V. In addition, it is seen from Figs. 6 and 7 that, in accordance with (7) and (8), the width of the steady-state soliton decreases, and the velocity  $w$  increases with increasing amplitude.

Let us estimate the extent to which the amplitudes of the steady-state solitons are close to the limiting amplitude  $\phi_m$  (1). The measured  $\phi_m = 2$  kV and  $w = 3.3 \times 10^9$  cm/sec yield  $\Phi_m = 0.65$ , i.e., the amplitudes of the observed solitons did not reach their maximum value.

<sup>1</sup>B. N. Rutkevich, A. V. Pashchenko, V. D. Fedorchenko, and V. I. Muratov, Zh. Tekh. Fiz. 42, 493 (1972) [Sov. Phys. Tech. Phys. 17, 391 (1972)].

<sup>2</sup>H. Ikezi, P. J. Barrett, R. W. White, and A. I. Wong, Phys. Fluids 14, 1997 (1971).

<sup>3</sup>S. I. Krivoruchko, Ya. B. Fainberg, V. D. Shapiro, and V. I. Shevchenko, Pis'ma Zh. Eksp. Teor. Fiz. 17, 344 (1973) [JETP Lett. 17, 244 (1973)].

<sup>4</sup>S. I. Krivoruchko, Ya. B. Fainberg, V. D. Shapiro, and V. I. Shevchenko, Zh. Eksp. Teor. Fiz. 67, 2092 (1974) [Sov. Phys. JETP 40, 1039 (1975)].

<sup>5</sup>V. D. Fedorchenko, Yu. P. Mazalov, A. S. Bakal', A. V. Pashchenko, and B. N. Rutkevich, Pis'ma Zh. Eksp. Teor. Fiz. 18, 477 (1973) [JETP Lett. 18, 281 (1973)].

<sup>6</sup>V. I. Kurilko and A. I. Tolstoluzhskii, Zh. Tekh. Fiz. 44, 1418 (1974) [Sov. Phys. Tech. Phys. 19, 887 (1975)].

Translated by J. G. Adashko